



Pharmacokinetics and Pharmacodynamics of Rusfertide, a Hepcidin Mimetic, Following Subcutaneous Administration of a Lyophilized Powder Formulation in Healthy Volunteers

Nishit B. Modi¹ · Sarita Khanna¹ · Sneha Rudraraju¹ · Frank Valone¹

Accepted: 31 October 2024 / Published online: 15 November 2024
© The Author(s) 2024

Abstract

Background and Objective Hepcidin, an endogenous peptide hormone, binds to ferroportin and is the master regulator of iron trafficking. Rusfertide, a synthetic peptide, is a potent hepcidin mimetic. Clinical studies suggest rusfertide may be effective in the treatment of polycythemia vera. This study investigated the dose-ranging pharmacokinetics, pharmacodynamics, and safety of a lyophilized formulation of rusfertide.

Methods A randomized open-label crossover study was conducted in two groups of healthy adult subjects to evaluate the safety, tolerability, pharmacokinetics, and pharmacodynamics of subcutaneous rusfertide doses that ranged from 10 to 60 mg of a lyophilized formulation and 20 mg of an aqueous prefilled syringe formulation that were used in clinical trials.

Results Rusfertide showed a rapid initial absorption. Median time to peak plasma concentrations for the lyophilized formulation was 24 h for doses of 10–30 mg and 2–4 h for doses of 45 and 60 mg. Mean terminal half-life ranged from 19.6 to 57.1 h. Rusfertide peak concentration and area under the concentration–time curve increased with an increasing dose, but in a less than dose-proportional manner. Metabolites M4 and M9 were identified as major metabolites. At the rusfertide 20-mg dose, the lyophilized formulation had an area under the concentration–time curve from time zero to infinity approximately 1.5-fold higher than the aqueous formulation. The elimination half-life was comparable for the two formulations. Dose-related decreases in serum iron and transferrin-iron saturation were seen following rusfertide treatment. The majority of treatment-emergent adverse events were mild; treatment-related treatment-emergent adverse events seen in $\geq 10\%$ of subjects were injection-site erythema and injection-site pruritus.

Conclusions Rusfertide was well tolerated; the pharmacokinetic and pharmacodynamic results indicate that lyophilized rusfertide is suitable for once-weekly or twice-weekly administration.

Plain Language Summary

Hepcidin is a natural peptide hormone produced by the liver that is responsible for iron homeostasis. Rusfertide is a potent peptide mimetic of hepcidin that is being investigated for the treatment of polycythemia vera. This trial was conducted in two groups of healthy subjects to describe the pharmacokinetics and pharmacodynamics of subcutaneous rusfertide. Doses of 10–60 mg of a lyophilized powder formulation and 20 mg of an aqueous formulation were studied in a randomized manner. Following subcutaneous dosing, maximum plasma concentration and exposure measured by area under the concentration–time curve increased with dose but in a less than proportional manner. Rusfertide reduced serum iron and transferrin-iron saturation in a dose-related manner. Rusfertide was generally well tolerated. Side effects seen in more than 10% of subjects that were considered possibly related to treatment were injection-site redness and itching.

Sneha Rudraraju: Affiliation at the time the trial was conducted.

✉ Nishit B. Modi
n.modi@ptgx-inc.com

¹ Protagonist Therapeutics, Inc., 7575 Gateway Blvd, Suite 110, Newark, CA 94560-1160, USA

Key Points

Rusfertide is a potent peptide mimetic of the natural peptide hormone hepcidin. Rusfertide is being investigated for the treatment of polycythemia vera. Following subcutaneous administration of rusfertide over a dose range of 10–60 mg in healthy subjects, peak plasma concentration and area under the concentration–time curve increased with dose but in a less-than dose-proportional manner.

Rusfertide resulted in reduction in serum iron and transferrin-iron saturation with maximum reduction noted approximately 24–48 h post-dose. The effect increased with dose with effects sustained up to 72 h at higher doses.

Rusfertide was generally well tolerated in healthy volunteers. Adverse effects noted in at least 10% of subjects that were considered possibly related to treatment were injection-site erythema and injection-site pruritus.

1 Introduction

Polycythemia vera (PV) is a chronic myeloproliferative neoplasm driven by activating mutations in the Janus kinase 2 gene that results in unrestrained erythrocytosis and increased hematocrit and hemoglobin concentrations, placing patients at an increased risk of thrombotic events and mortality [1–3]. Treatment guidelines for PV recommend maintaining hematocrit below 45% to minimize thromboembolic and cardiovascular risk [4–6]. Treatment is generally initiated with low-dose aspirin and a periodic therapeutic phlebotomy to maintain a hematocrit <45%. Pegylated interferon alpha-2a or ropeginterferon alfa-2b may be considered in patients aged younger than 60 years and those without a history of a thrombotic event, who have low-risk disease, and who have frequent phlebotomies, severe pruritus, persistent symptoms, or symptomatic splenomegaly [7]. Patients with a high-risk disease defined as those aged older than 60 years or with a history of thrombosis are treated with hydroxyurea, a Janus kinase 2 inhibitor, or pegylated interferon alpha. However, current treatments are often ineffective for maintaining hematocrit levels in the recommended range. Among high-risk patients with PV, only 25% had hematocrit levels consistency below 45%, while 7% had hematocrit values always >50% [8].

Iron is an essential trace element for nearly every living organism and the most abundant trace element in humans

[9, 10]. The human body contains approximately 3–4 g of iron, with most in erythrocyte hemoglobin (~ 2–3 g) [9]. Hepcidin, a 25-amino acid peptide hormone synthesized primarily by hepatocytes, is the master regulator of systemic iron homeostasis [11, 12]. Hepcidin inhibits iron absorption in the proximal small intestine [13] and controls iron export to the plasma by inducing degradation of the iron exporter ferroportin in macrophages and hepatocytes [14, 15]. Iron and hepcidin regulate each other in a classical endocrine feedback loop. When hepcidin levels are low, iron enters the blood compartment; when hepcidin levels are high, ferroportin is internalized and iron is trapped in enterocytes, macrophages, and hepatocytes [16], and can lead to iron-restricted anemia. This observation suggests that hepcidin could be a therapeutic useful for treating conditions of excessive erythropoiesis, such as PV. However, synthesis of full-length hepcidin is relatively inefficient, and the short plasma half-life of hepcidin due to proteolysis and renal clearance limits its use as a therapeutic agent [17, 18].

Rusfertide (also known as PTG-300) is a synthetic peptide mimetic of the natural peptide hormone hepcidin that is being investigated as a potential treatment for PV. The pharmacokinetic (PK) and pharmacodynamic (PD) characteristics of rusfertide make it suitable as a therapeutic. In a cell-based ferroportin internalization assay, the EC₅₀ values of hepcidin and rusfertide were 67.8 and 6.12 nM, respectively [19]. Subcutaneous (SC) administration of rusfertide in cynomolgus monkeys resulted in a dose-dependent reduction of serum iron and anemia. A single SC injection of rusfertide 0.3 mg/kg in cynomolgus monkeys resulted in a maximum reduction in serum iron of 54.9% 24 h post-dose. Maximum rusfertide plasma concentrations (172 ± 31 nM) were noted at 8 h post-dose, and the estimated elimination half-life was approximately 24 h [20].

Rusfertide has shown efficacy in PV in phase II studies, reducing elevated hematocrit levels [21] and maintaining hematocrit levels < 45% in patients with PV [22] and recent reports have demonstrated that rusfertide treatment can provide long-term control of hematocrit [23]. Rusfertide is currently being investigated in a randomized, double-blind, placebo-controlled phase III study in patients with PV [24]. In addition, a proof-of-concept clinical study has indicated that rusfertide was also well tolerated and effective for controlling iron overload in patients with HFE-related hemochromatosis [25].

The dose-ranging pharmacokinetics and pharmacodynamics of an aqueous prefilled syringe formulation of rusfertide that was used in phase II studies in patients with PV has been reported previously [26]. Following SC administration of the aqueous formulation in healthy subjects, rusfertide plasma concentrations are noted within 1 h of dosing, and peak concentration (C_{\max}) occurred at a

median of approximately 2–24 h. Following the peak, rusfertide concentrations for the aqueous formulation decreased with an elimination half-life of 17.9–52.5 h. Peak plasma concentration and area under the concentration–time curve increased with rusfertide dose but less than dose proportionally. Corresponding with the pharmacokinetics, dose-related PD decreases in serum iron and transferrin-iron saturation (TSAT) were noted.

While the aqueous formulation was suitable for phase II safety and efficacy studies, it has limited stability and was not considered suitable for large global studies. Lyophilization is frequently used to prepare peptides in a solid state, increasing chemical and physical stability [27, 28]. The present study evaluated the dose-ranging pharmacokinetics, pharmacodynamics, and tolerability of a lyophilized formulation of rusfertide compared to the aqueous formulation.

2 Methods

The trial protocol, consent form, and other information provided to participants were reviewed and approved by the Advarra Institutional Review Board (Pro00059393, Approval 23 November, 2021). The trial was conducted in compliance with the ethical principles originating in or derived from the Declaration of Helsinki and in compliance with all International Council for Harmonization Good Clinical Practice Guidelines, and all study procedures were conducted by scientifically and medically qualified personnel. Written informed consent was obtained from each participant before any study-specific activity was performed.

2.1 Study Design

In this randomized, open-label, dose-ranging, four-way crossover study, the pharmacokinetics, pharmacodynamics, safety, and tolerability of single doses of rusfertide were evaluated in two groups of 16 healthy subjects at a single US site using two formulations: a lyophilized powder formulation for reconstitution and an aqueous formulation in a pre-filled syringe. The study was conducted between January and March 2022. Subjects in Group 1 received SC doses of rusfertide 20, 30, and 60 mg as a lyophilized formulation and 20 mg as the aqueous formulation in a randomized manner. Subjects in Group 2 received SC doses of rusfertide 10, 20, and 45 mg as a lyophilized formulation and 20 mg as an aqueous formulation in a randomized manner. Subjects in both groups received 20 mg of both formulations. This study design was chosen to provide a direct comparison of the 20-mg dose of both formulations and to limit the number of treatments in each subject to four treatments to reduce the number of dropouts. The lyophilized formulation was

reconstituted by clinical staff using the accompanying diluent and administered to subjects. All dose injections were 0.5 mL in volume, administered subcutaneously to the abdomen, 2 inches from the navel, with a washout period of at least 13 days between treatments. This study in healthy subjects did not meet the definition of “applicable clinical trial,” and it was not required to be registered on clinicaltrials.gov.

2.2 Study Population

Eligible subjects were male or female, aged 18–65 years, inclusive, in good general health with no significant abnormalities on a physical examination, with no laboratory values considered clinically significant by the investigator, and a body mass index between 18 and 32 kg/m². Women were surgically sterile, postmenopausal, or, if of childbearing potential, agreed to use medically acceptable contraception (< 1% annual failure rate) during the study and for 30 days after the last dose of study medication. Key exclusion criteria included a history of clinically significant endocrine, neurological, gastrointestinal, cardiovascular, hematological, hepatic, immunological, renal, respiratory, or genitourinary abnormalities or disorders, non-invasive squamous cell carcinoma of the skin (unless adequately treated), a history of invasive malignancies within the previous 5 years (except localized cured prostate or cervical cancer), a history of severe allergic or anaphylactic reactions, supine blood pressure outside 90–139 mm Hg systolic and 50–89 mm Hg diastolic, or a heart rate greater than 100 beats per minute.

2.3 Dose Selection

Single doses of 10, 20, 30, 45, and 60 mg of the lyophilized rusfertide formulation were chosen for this trial to study the complete range of rusfertide dose strengths that are included in the larger phase III safety and efficacy study. The 20-mg aqueous formulation dose strength was included for comparison with the 20-mg lyophilized formulation because 20 mg is the recommended starting dose of rusfertide.

2.4 Pharmacokinetic (PK) Assessments

To assess the PK profile of rusfertide and its metabolites, plasma samples were collected pre-dose, and at 1, 2, 4, 8, 12, 24, 36, 48, 72, 96, 120, 144, 168, 192, and 216 h following dosing. Subjects were released from the clinical unit following the 48-h sample, with subsequent samples collected at outpatient visits. Plasma samples were isolated by centrifugation and stored at –70 °C within 60 min of collection.

Twelve subjects had detectable pre-dose rusfertide plasma concentrations during at least one of the treatments. For these subjects, prior to conducting PK analyses, the plasma concentrations were corrected assuming a first-order

elimination using the average elimination half-life estimated following intravenous administration of rusfertide from a separate trial.

Pharmacokinetic parameters were estimated by non-compartmental methods using Phoenix WinNonlin version 8.3 (Certara, Princeton, NJ, USA). Peak plasma concentration and time to C_{\max} (T_{\max}) were observed values. The elimination rate was estimated from the slope of the least-squares regression on the terminal log-linear phase. Area under the concentration–time curve (AUC) from time zero to the last quantifiable concentration was estimated by a linear trapezoidal method and was extrapolated to infinity (AUC_{inf}) by dividing the last quantifiable concentration by the elimination rate. To allow a comparison across treatments in this crossover study conducted in two groups of subjects, summaries of PK data are based on the group of subjects that completed all treatments.

The PK analysis set included all subjects who received at least one dose of study medication and had data for at least one PK parameter. Pharmacokinetic completers were subjects who had received all four study doses. Pharmacokinetic parameters were summarized using descriptive statistics.

2.5 Bioanalytical Methods

Plasma concentrations of rusfertide and metabolites (M1, M4, M6, M9) were determined using two liquid chromatography/tandem mass spectrometry methods that were performed under Good Laboratory Practice guidelines: a multi-analyte liquid chromatography/tandem mass spectrometry method for rusfertide, M1, M6, and M9; and a separate liquid chromatography/tandem mass spectrometry method for M4. The bioanalytical methods were developed in accordance with current ICH guidelines on bioanalytical method validation and study sample analysis [29].

The analytical methods for determination of rusfertide and M4 concentrations were validated for selectivity, linearity, reproducibility, recovery, precision, and accuracy over the concentration range of 2.00–500 ng/mL and qualified for M1, M6, and M9 over a concentration range of 3.00–750 ng/mL.

Quality-control cumulative accuracy (percent relative error) was –2.0 to 3.0% for rusfertide and –12.6% to 6.7% for the metabolites. Cumulative precision (percent coefficient of variation) was $\leq 3.8\%$ for rusfertide and $\leq 11.5\%$ for the metabolites.

2.6 Pharmacodynamic (PD) Assessments

The PD effects of rusfertide were assessed by measuring serum iron and transferrin-iron saturation. Samples were collected pre-dose, and at 4, 8, 24, 48, 72, 96, 120, 144, and 168 h following dosing.

Pharmacodynamic effects on serum iron and TSAT were summarized by estimating the area under the PD effect-time curve (AUEC) from zero to 168 h. The rusfertide AUC–AUEC relationship for serum iron and for TSAT was investigated. All subjects who received at least one dose of study medication and had AUEC data for at least one PD endpoint were included in the PD analyses.

2.7 Safety Assessments

Safety evaluations were based on adverse events (AEs) and the use of concomitant medications, as well as clinical laboratory test values, physical examinations, vital sign measurements, and electrocardiogram findings, each assessed at pre-specified timepoints. Adverse event occurrences and concomitant medication usage were recorded throughout the study. Physical examinations were conducted at screening and at the end of the study. Clinical laboratory assessments, including hematology, clinical chemistry, coagulation, and urinalysis, were conducted at check-in and at 4 and 48 h following dosing, and at the end of the study. Electrocardiogram measurements and vital sign recordings were made pre-dose, and at 2, 4, 8, 12, 24, 48, 72, 120, and 216 h following dosing and at the end of the study.

All participants who received at least one dose of study medication were included in the safety analyses. Adverse events were considered treatment emergent if they started or worsened after the first administration of treatment. Severity grading of AEs was done according to the Common Terminology Criteria for Adverse Events Version 5.0 [30]. Adverse events were coded using the Medical Dictionary for Regulatory Activities (Version 24.1) and evaluated by the principal investigator. The intensity of the AE was rated as mild, moderate, severe, life threatening, or fatal, and the relationship between the AE and study medication was indicated as not related, unlikely related, possibly related, or related.

2.8 Immunogenicity Assessments

Serum samples were collected prior to the first rusfertide dose and at the end of study participation for determination of rusfertide antidrug antibodies. Serum antidrug antibodies were examined via a validated enzyme-linked immunosorbent assay using a three-tiered approach (screening, confirmation, and titration analysis).

2.9 Statistical Analyses

As this study was not a bioequivalence study, no formal sample size estimations were performed in this single-dose trial. The number of participants enrolled in each group was consistent with the customary size employed in PK studies.

and was expected to allow a meaningful assessment of pharmacokinetics and pharmacodynamics and clinical judgment of safety and tolerability.

Statistical analyses were performed using SAS version 9.4 (SAS Institute, Cary, NC, USA). The PK-PD analysis was conducted using GraphPad Prism version 10.3.1 for Windows (GraphPad Software, Boston, MA, USA). Dose proportionality of C_{\max} and AUC_{\inf} for the rusfertide lyophilized formulation was assessed based on a power model [$Y = \alpha \cdot (\text{dose})^\beta$] as described by Gough et al. [31] using the modification by Smith et al. [32]. In the power model, Y is the PK parameter, α is the expected value of Y for a dose of unity, and β is the proportionality exponent. A mixed-effects model, allowing for random between-subject variability in α and β , was implemented to estimate the proportionality constant and its 90% confidence interval (CI). Dose proportionality was declared if the calculated 90% CI lay within the acceptance range [$1 + \ln(\Theta_L)/\log(R)$, $1 + \ln(\Theta_H)/\log(R)$], where Θ_L and Θ_H are the lower and upper limits of the CI (0.8 and 1.25, respectively) and R is the ratio between the highest and lowest doses ($R = 6$ in this study).

3 Results

3.1 Subject Disposition

Two groups of 16 subjects were enrolled. Eleven subjects completed all four treatments in Group 1; one subject was withdrawn for protocol non-compliance, one withdrew because of a family emergency, and three discontinued because of AEs. One subject experienced injection-site erythema, induration, and itching, another experienced injection-site erythema, and a third reported urticaria. Fourteen subjects completed all four treatments in Group 2; one subject discontinued because of coronavirus disease 2019 infection and another withdrew to care for a relative with coronavirus disease 2019 infection. Overall, 25 of 32 subjects enrolled (78.1%) completed the study.

3.2 Demographics and Baseline Characteristics

The demographics and baseline characteristics of subjects in the two groups are summarized in Table 1. Subjects ranged in age from 28 to 63 years and were equally distributed by sex. The majority of subjects were Black or African American (56%), and 31% were White. The mean body mass index was 27.2 kg/m² (range 21.2–30.9 kg/m²). Subject demographics were generally well balanced between the two groups.

3.3 Pharmacokinetics

3.3.1 Rusfertide

The mean rusfertide plasma concentration–time profiles following single doses of rusfertide for both formulations are presented in Fig. 1. Semi-logarithmic profiles are presented in Fig. 1 of the Electronic Supplementary Material (ESM). A summary of rusfertide pharmacokinetics is presented in Table 2. Following SC administration, rusfertide concentrations were detected within 1 h of dosing, with plasma concentrations increasing and sustained over time. The median T_{\max} for rusfertide for the lyophilized formulation was 24 h for doses up to 30 mg, and 2–4 h for the 45- and 60-mg doses. The median T_{\max} for rusfertide for the 20-mg dose of the aqueous formulation was 1 h. For doses of 20 mg and higher of the lyophilized formulation, there was a rapid increase in rusfertide concentration; in some instances, a dual peak could be seen in the rusfertide concentration profile. Dose-related increases were seen in rusfertide C_{\max} and AUC. The mean elimination half-life for rusfertide ranged from 19.6 to 57.1 h. Mean apparent plasma clearance of rusfertide for the lyophilized formulation ranged from approximately 0.63 to 1.5 L/h, with apparent clearance increasing with an increasing rusfertide dose. The apparent clearance for rusfertide 20 mg as the aqueous formulation was 1.5 L/h compared with an apparent clearance of 0.98 L/h for the lyophilized formulation. The rusfertide 20-mg lyophilized formulation had an approximate 1.5-fold higher AUC_{\inf} exposure than the 20-mg dose of the aqueous formulation.

Rusfertide dose proportionality was evaluated for the lyophilized formulation doses using a power analysis (Table 3; Fig. 2). Following single-dose administration of rusfertide, rusfertide C_{\max} and AUC_{\inf} values increased in a less than dose-proportional manner. The proportionality exponent (β) for C_{\max} and AUC_{\inf} were less than unity. The acceptance interval for dose proportionality for this study was (0.8755, 1.12450). The 90% CI of β (Table 3) was not wholly contained within this interval, indicating a less than dose-proportional increase in C_{\max} and AUC_{\inf} .

3.3.2 Metabolites M1, M4, M6, and M9

Metabolite M9 exposure was 24.9% of all drug-related exposure (AUC) for the aqueous formulation and ranged from 25.4 to 32.6% of all drug-related exposure for the lyophilized formulation (Table 2). Metabolite M4 AUC exposure was 20.9% of all drug-related exposure in the aqueous formulation, while for the lyophilized product, the percentage of M4 exposure relative to all drug-related exposure increased with

Table 1 Subject demographics and baseline characteristics

	Group 1 (N = 16)	Group 2 (N = 16)	Total (N = 32)
Age, years	41.6 ± 9.7	44.3 ± 10.5	42.9 ± 10.0
Sex, n (%)			
Male	9 (56)	7 (44)	16 (50)
Female	7 (44)	9 (56)	16 (50)
Race, n (%)			
Black or African American	10 (63)	8 (50)	18 (56)
White	4 (25)	6 (38)	10 (31)
American Indian or Alaska native	1 (6)	0	1 (3)
Other	1 (6)	2 (13)	3 (9)
Weight, kg	82.0 ± 10.2	76.1 ± 7.2	79.0 ± 9.2
BMI, kg/m ²	27.5 ± 2.6	26.8 ± 2.8	27.2 ± 2.7

Data are presented as mean ± standard deviation unless otherwise stated

BMI body mass index

dose, with a range from 1.9% at 10 mg to 18.5% at 60 mg. Therefore, M9 is considered a major metabolite ($\geq 10\%$) and conservatively, M4 is also considered a major metabolite for this single-dose study. Across all the dose levels, T_{\max} of M4 and M9 appeared later than that of rusfertide. The elimination half-lives for M4 and M9 were comparable to that for rusfertide. Metabolites M1 and M6 were detected only sporadically and are considered minor metabolites, comprising $< 1\%$ of all drug-related AUC.

3.4 Pharmacodynamics

3.4.1 Serum Iron

A dose-related acute decrease in serum iron levels was seen following SC rusfertide (Fig. 3A). Peak decrease in serum iron was noted at 24 h and at higher doses, the decrease was sustained until 72 h after which serum iron levels started to return to baseline. A dose-related recovery of the PD effect to baseline was noted, with a faster recovery following 10 mg and a slower recovery following 60 mg. At 10 mg, there was an overshoot in the effect above baseline, reflective of the transient effect at this dose and the general variability in the response. The 20-mg dose of the lyophilized formulation had a similar reduction in serum iron compared with the 20-mg aqueous formulation with a similar return to baseline (Fig. 3A).

3.4.2 Transferrin-Iron Saturation (TSAT)

Consistent with the effects seen with serum iron, TSAT decreased following SC administration, with peak effects noted at 24–48 h (Fig. 3B), and the effect was sustained at the higher doses. Following the nadir, TSAT levels

returned towards baseline and for the lower doses of 10 and 20 mg, the TSAT levels were essentially back to baseline by 168 h. The 20-mg doses of the lyophilized formulation and the aqueous formulation had a similar PD effect on TSAT.

3.5 Pharmacokinetic (PK) and Pharmacodynamic (PD) Correlation

The PD effects on serum iron and TSAT generally matched the rusfertide plasma concentration profile. The relationship between AUEC for serum iron and for TSAT and rusfertide AUC was well described by a linear relationship (Fig. 4). A comparison of the y-intercept and slope for the linear relationships for the lyophilized formulation and the aqueous formulation for serum iron and for TSAT indicated that the slopes and intercepts between the two formulations were not significantly different ($p = 0.427$ and 0.503 for slope and intercept, respectively, for serum iron, and $p = 0.195$ and $p = 0.379$ for slope and intercept, respectively, for TSAT) and a single linear relationship could be used for both formulations (Table 4). Examining the relationship for serum iron and for TSAT using data just for the 20-mg dose for both formulations showed similar findings that a single linear relationship could be used for both formulations (Fig. 2 and Table 1 of the ESM).

3.6 Safety and Tolerability

Sixteen (50%) of the 32 subjects enrolled in the study experienced a treatment-emergent AE (TEAE) [Table 5]. No serious TEAEs were reported. Most TEAEs were mild or moderate in severity. One subject in each of the 20-mg

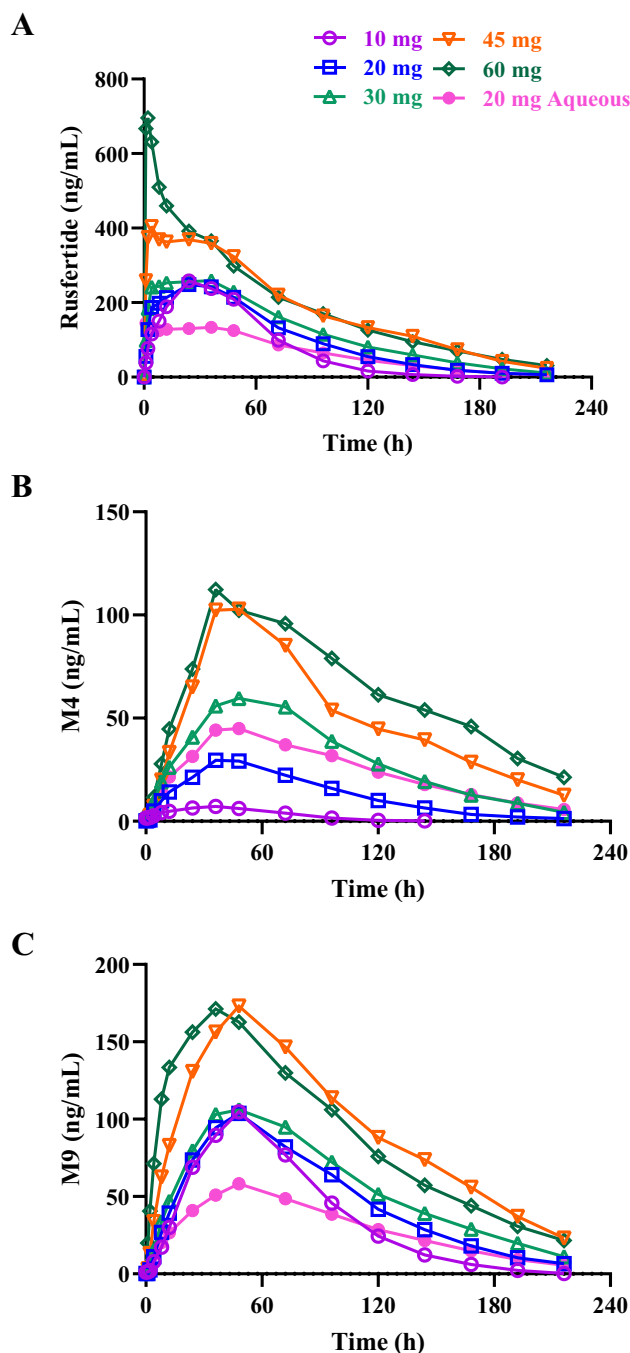


Fig. 1 Mean plasma concentration–time profile for **A** rusfertide, **B** metabolite M4, and **C** metabolite M9. *h* hours

aqueous formulation and the 60-mg lyophilized formulation experienced injection-site erythema that was considered severe. Three subjects experienced treatment-related AEs that led to discontinuation of treatment; injection-site erythema, induration, and pruritus in one subject, injection-site erythema in a second subject, and urticaria in the third subject. Treatment-emergent AEs reported in at least two subjects that were considered treatment related

were injection-site erythema (13%), injection-site pruritus (13%), injection-site induration (9%), and injection-site pain (9%). Overall, 9 of 32 subjects (28%) reported injection-site reactions.

There was no relationship between the severity of AEs and dose. Overall, there was no difference in the AE profile between the two formulations at the 20-mg dose. No consistent clinically meaningful changes were noted in the clinical laboratory results, vital signs, or electrocardiogram results.

3.7 Immunogenicity

A total of 58 samples were screened for the presence of anti-rusfertide antibodies in human serum. Of these, all samples except one were considered negative. One sample at the early termination visit from one subject, a 57-year-old man who discontinued the study after the second treatment, yielded an optical density value above the corresponding plate specific cut-off point with a positive titer of 507 units. Evaluation of the rusfertide concentrations in this subject did not indicate any difference in the exposure compared to other subjects. Apart from injection-site erythema following a 60-mg dose that led to treatment discontinuation, the subject also did not report any other TEAEs.

4 Discussion

Rusfertide, a peptide mimetic of the natural peptide hormone hepcidin, is currently under investigation for the treatment of PV. Clinical trials in healthy subjects and phase II trials in patients with PV or hemochromatosis used rusfertide as an aqueous formulation. In phase II trials in patients with PV, the aqueous formulation demonstrated significant efficacy in maintaining hematocrit < 45%, essentially eliminating the need for phlebotomies, and demonstrated long-term control of hematocrit [22, 23]. While the aqueous formulation was suitable for phase II studies, this formulation was not considered suitable for phase III and long-term trials. A lyophilized formulation provides a longer shelf-life, allowing for global trials over a wider geographic temperature range. Lyophilization is often used as a means of improving the shelf-life of peptide and protein drugs that are frequently subject to instabilities because of the presence of water [27, 28]. The current study investigated the dose-ranging pharmacokinetics, pharmacodynamics, and safety of a lyophilized formulation of rusfertide (10–60 mg) and an aqueous formulation (20 mg) in healthy volunteers. The recommended starting dose of rusfertide for both formulations is 20 mg, supporting the use of this dose strength for comparison of the two formulations. In clinical practice, the dose of rusfertide is titrated for each subject to identify a dose that maintains hematocrit levels below 45%. The mean weekly rusfertide

Table 2 Pharmacokinetic parameters of rusfertide and metabolites M4 and M9 following subcutaneous dosing

	Lyophilized formulation					Aqueous formulation
	10 mg (<i>N</i> = 14)	20 mg (<i>N</i> = 25)	30 mg (<i>N</i> = 11)	45 mg (<i>N</i> = 14)	60 mg (<i>N</i> = 11)	20 mg (<i>N</i> = 25)
Rusfertide						
C_{\max} (ng/mL)	261 ± 64.4	264 ± 73.9	287 ± 90.0	460 ± 106	776 ± 842	171 ± 52.0
T_{\max} (h) ^a	24 (24, 48)	24 (4, 48)	24 (4, 36)	4 (2, 48)	2 (1, 12)	1 (1, 72)
AUC _{inf} (ng·h/mL)	16,400 ± 2990	21,600 ± 5130	26,400 ± 6800	40,600 ± 8900	47,000 ± 18200	14,300 ± 4580
$t_{1/2}$ (h)	19.6 ± 5.22	28.6 ± 11.3	26.6 ± 6.39	33.0 ± 18.4	57.1 ± 73.0	33.5 ± 19.3
CL/F (L/h)	0.629 ± 0.123	0.979 ± 0.245	1.20 ± 0.299	1.16 ± 0.242	1.48 ± 0.629	1.54 ± 0.508
V_z/F (L)	18.2 ± 7.54	40.5 ± 20.1	47.3 ± 18.4	54.2 ± 32.0	104 ± 84.8	79.2 ± 59.7
Ratio of rusfertide AUC _{inf} to total AUC _{inf} (%)	65.5 ± 3.96	61.7 ± 4.53	58.2 ± 4.16	55.2 ± 4.55	55.2 ± 4.96	53.7 ± 3.66
M4						
C_{\max} (ng/mL)	7.67 ± 5.62	31.3 ± 17.1	63.4 ± 33.0	110 ± 68.8	119 ± 80.2	49.5 ± 21.8
T_{\max} (h) ^a	36 (8, 48)	48 (36, 96)	48 (36, 72)	48 (36, 144)	48 (36, 96)	48 (36, 144)
AUC _{inf} (ng·h/mL)	–	2960 ± 1130 ^b	6760 ± 2640	12,000 ± 4800 ^c	17,700 ± 6210 ^d	5750 ± 1720 ^f
$t_{1/2}$ (h)	–	36.6 ± 14.9 ^b	33.9 ± 8.99	36.4 ± 17.4 ^c	37.5 ± 17.1 ^d	34.1 ± 12.3 ^f
Ratio of M4 AUC _{inf} to Total AUC _{inf} (%)	1.90 ± 1.74	8.39 ± 3.82	14.6 ± 4.35	15.5 ± 7.03	18.5 ± 7.78	20.9 ± 5.87
M9						
C_{\max} (ng/mL)	105 ± 27.1	105 ± 33.2	113 ± 53.8	177 ± 46.9	197 ± 149	59.5 ± 27.6
T_{\max} (h) ^a	48 (36, 48)	48 (24, 72)	48 (36, 96)	48 (24, 144)	36 (12, 48)	48 (36, 96)
AUC _{inf} (ng·h/mL)	8260 ± 1670	10,700 ± 2930	12,800 ± 4450	21,700 ± 5210	21,800 ± 9360 ^e	6830 ± 2300
$t_{1/2}$ (h)	25.4 ± 4.79	32.8 ± 8.53	36.8 ± 9.52	39.8 ± 15.5	45.2 ± 16.0 ^e	41.0 ± 15.8
Ratio of M9 AUC _{inf} to Total AUC _{inf} (%)	32.6 ± 4.08	29.7 ± 4.44	26.8 ± 4.11	28.7 ± 4.23	25.4 ± 6.30	24.9 ± 3.53

Data are mean ± standard deviation unless otherwise noted

AUC area under the concentration–time curve, CL/F apparent clearance, C_{\max} peak plasma concentration, T_{\max} time to maximum concentration, $t_{1/2}$ elimination half-life, total AUC sum of AUC for rusfertide and all metabolites, V_z/F apparent volume of distribution

^aMedian (minimum, maximum)

^b*N* = 23

^c*N* = 12

^d*N* = 8

^e*N* = 10

^f*N* = 20

Table 3 Rusfertide proportionality analysis

Pharmacokinetic parameter	Proportionality exponent (β) value (SE)	90% confidence interval
C_{\max} (ng/mL)	0.683 (0.0868)	0.539, 0.828
AUC _{inf} (h·ng/mL)	0.766 (0.0580)	0.669, 0.862

AUC_{inf} area under the concentration–time curve from time zero to infinity, C_{\max} peak plasma concentration, SE standard error

dose in subjects who completed the open-label dose-titration phase of the phase II REVIVE study was 41.3 mg [33], supporting the dose range of 10–60 mg selected for the current study. Because rusfertide is titrated to effect, the current PK and PD investigation was not designed as a bioequivalence

trial and rather was intended to provide an understanding of the improvement in the rusfertide exposure from the lyophilized formulation relative to the previously studied aqueous formulation.

Following SC administration, rusfertide plasma concentrations were noted within 1 h, the first sampling timepoint. Median peak concentrations occurred 24–48 h following dose administration for the 10–30-mg doses of the lyophilized formulation and occurred earlier for the 45- and 60-mg doses. The SC absorption of rusfertide is extended, possibly a result of dual absorption pathways, which in combination with a modestly long elimination half-life results in sustained plasma concentrations and a delayed T_{\max} . An earlier T_{\max} is noted at higher doses, possibly reflecting an increase in the fraction of rusfertide absorbed

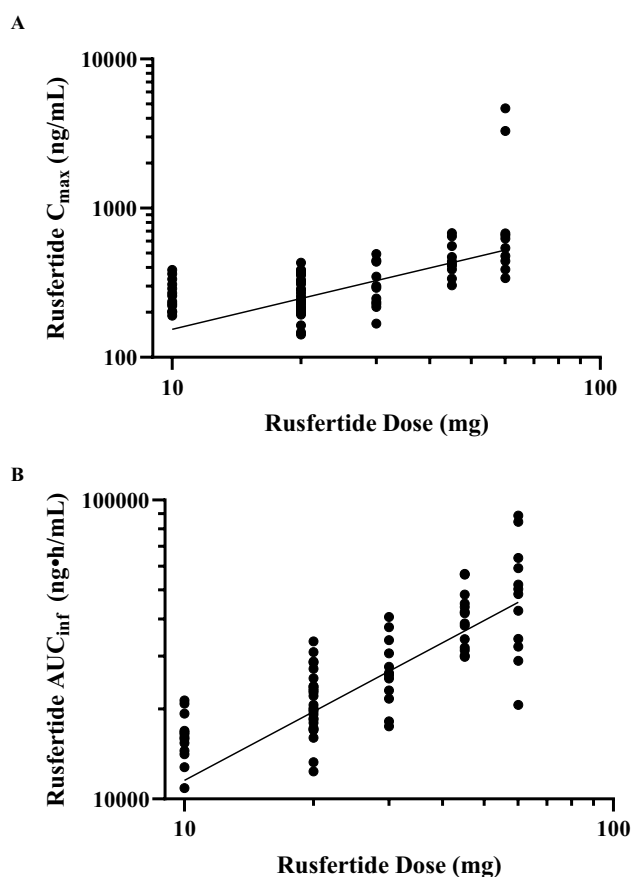


Fig. 2 Dose proportionality of rusfertide pharmacokinetics for the lyophilized formulation. **A** Peak concentration (C_{max}) and **B** area under the plasma concentration–time curve from time zero to infinity (AUC_{inf}) [log–log scale]

rapidly compared with a portion that may be absorbed more slowly at lower doses.

Similar to a previous study with the aqueous formulation [26], a less-than-proportional increase in exposure (C_{max} and AUC) was seen for the lyophilized formulation over the dose range of 10–60 mg in the current study. The mean elimination half-life for the lyophilized formulation was 19.6–57.1 h. There was a trend of increasing apparent clearance and apparent volume of distribution with an increasing rusfertide dose, which may explain the less-than-proportional increases in C_{max} and AUC. Rusfertide likely follows clearance through linear and non-linear (saturable, potentially target-mediated drug disposition) mechanisms. The increase in apparent clearance and volume of distribution with increasing dose may be reflective of the saturation of the non-linear clearance, resulting in an increase in the amount of free drug and a higher rate of clearance. This non-linear clearance may be reflective of target-mediated drug disposition, which would be consistent with the mechanism of action of rusfertide with saturable binding to the ferroportin receptor. At lower doses, rusfertide may bind to ferroportin

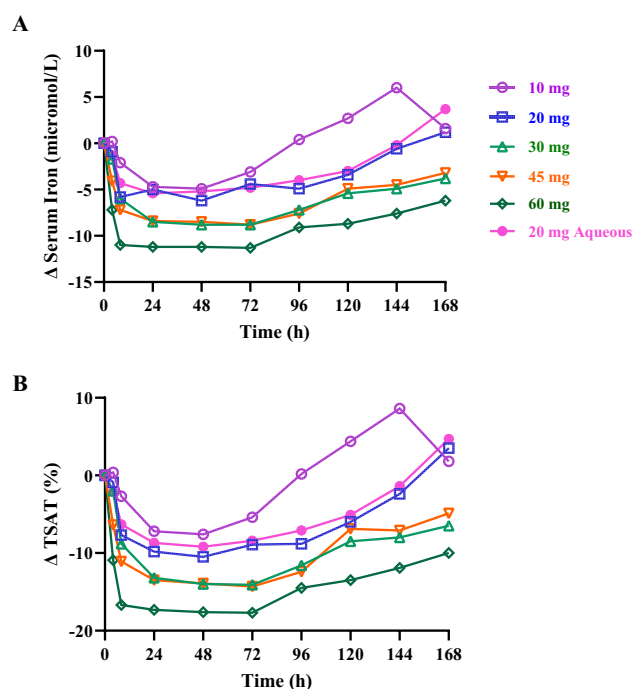


Fig. 3 Mean change from baseline in **A** serum iron profile and **B** transferrin-iron saturation (TSAT) following rusfertide administration. *h* hours

receptors, which remove the drug from the plasma circulation and leads to the shorter half-life. With increasing dose, ferroportin binding may become saturated, resulting in more free drug available for linear (non-saturable) clearance. This leads to the increased clearance at higher doses and may also reflect the true systemic elimination half-life of rusfertide. Alternatively, the increase in apparent clearance with an increasing dose may reflect differences in bioavailability or changes in metabolism with dose, especially M4.

Compared with the aqueous formulation, lyophilized rusfertide had an approximately 1.5-fold higher AUC at 20 mg. The reconstituted lyophilized formulation contains zinc acetate and mannitol, which may contribute to the improved PK behavior of this formulation. The addition of zinc has been shown to chelate trace amounts of free thiols that may form during the drug substance manufacturing process for peptides [34, 35]. Furthermore, zinc has been shown to have additional benefits as a formulation additive, aiding in the stabilization of peptides and contributing to bioavailability enhancements [36, 37].

Pharmacokinetics of the 20-mg dose of the rusfertide aqueous formulation was comparable to that noted in a previous study [26]. Although the lyophilized formulation resulted in higher C_{max} and AUC values compared with the aqueous formulation at 20 mg, there did not appear to be a difference in the PD effect on serum iron and TSAT at this dose level between the two formulations. We attribute this

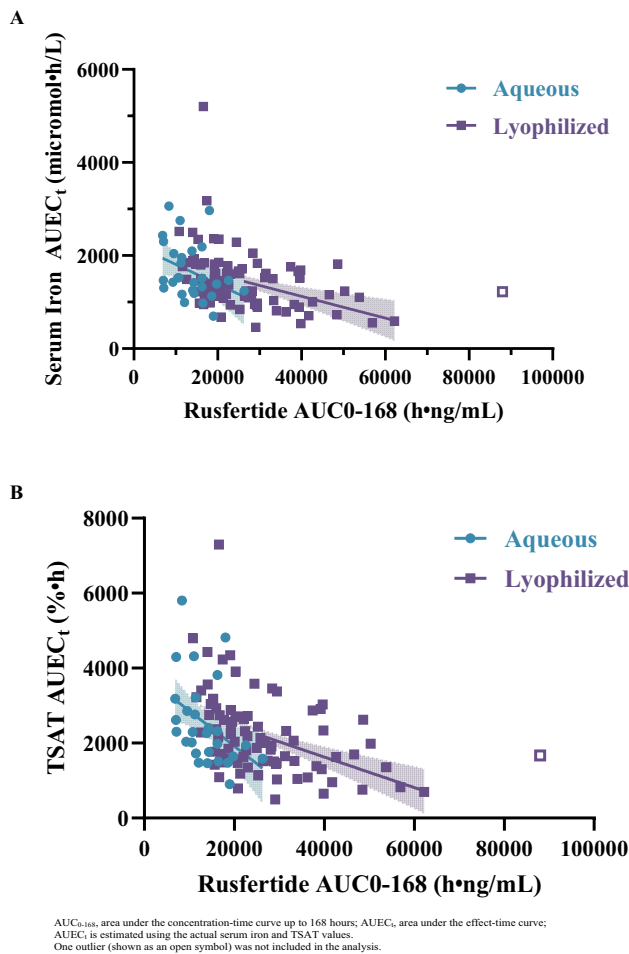


Fig. 4 Relationship between rusfertide area under the concentration–time curve (AUC) and **A** serum iron area under the pharmacodynamic effect–time curve (AUEC) and **B** transferrin-iron saturation (TSAT) AUEC for the lyophilized and aqueous formulation

Table 4 Summary of relationship between rusfertide area under the concentration–time curve and pharmacodynamic area under the effect curve for serum iron and transferrin-iron saturation

		Intercept	Slope	P-value for comparison
Serum iron	Aqueous	2235	– 0.04256	Slope: 0.4268 Intercept: 0.5030
	Lyophilized	2060	– 0.0234	
	Combined	2064	– 0.02452	
TSAT	Aqueous	3798	– 0.0939	Slope: 0.1945 Intercept: 0.3789
	Lyophilized	3257	– 0.04075	
	Combined	3283	– 0.04388	

TSAT transferrin-iron saturation

partly to the asymptotic concentration–effect relationship wherein the effect on change in serum iron and TSAT is similar for the two formulations up to approximately a rusfertide concentration of 130 ng/mL, the common range in rusfertide concentrations, above which there are smaller changes from baseline in the PD effects with further increases in the rusfertide concentration (Fig. 3 of the ESM).

M1 and M6 comprise < 1% of the total drug-related AUC and are considered minor metabolites. According to the metabolites in safety testing guidelines, M9, and conservatively M4, are considered major metabolites for the lyophilized formulation because their AUC values comprise > 10% of the total AUC [38]. At the 20-mg dose, rusfertide AUC_{inf} comprised 61.7% of the total drug-related AUC_{inf} for the lyophilized formulation and 53.7% for the aqueous formulation. M4 comprised 8.4% of the total drug-related AUC for the lyophilized formulation and 20.9% for the aqueous formulation. In contrast, there was a smaller difference in the M9 exposure between the two formulations; M9 comprised 29.7% of the total AUC for the lyophilized formulation and 24.9% for the aqueous formulation. Metabolites M4 and M9 have approximately 1.5-fold and 7.2-fold lower potencies, respectively, than rusfertide in a cell-based, in vitro ferroportin internalization assay. Taking the relative potency into account, based on the AUC_{inf} of rusfertide, M4 and M9, at 20 mg, rusfertide accounts for approximately 86% of the pharmacologic activity with the M4 and M9 metabolites accounting for 8% and 6% of the activity, respectively, for the lyophilized formulation.

Median time to peak concentration for both major metabolites, M4 and M9, occurred similar to or later than that of rusfertide, suggesting the absence of pre-systemic metabolism for these metabolites. Metabolites M4 and M9 had similar mean elimination half-lives as rusfertide, suggesting that these two metabolites follow formation rate-limited pharmacokinetics.

There is increasing recent interest in the use of hepcidin, mini-hepcidins [39], and targeting transmembrane serine protease 6 using antisense nucleotides [40–42], small interfering RNA [1, 43], or monoclonal antibodies [44, 45] for iron overload disorders. Hepcidin is reported to have a rapid clearance, primarily through renal excretion and reabsorption, which limits its use as a therapeutic [46]. Rusfertide appears to have favorable PK and PD characteristics compared with some other investigational agents that have effects on the ferroportin receptor.

Subcutaneous administration of LJPC-401, a synthetic hepcidin, in healthy subjects resulted in peak concentrations at approximately 2 h and the mean terminal half-life ranged from ~ 3 to 11 h [47]. Mean maximum reduction in serum iron with LJPC-401 occurred 4–8 h post-dose with

Table 5 Summary of TEAEs in two or more subjects overall following subcutaneous dosing of rusfertide as a lyophilized formulation and as a pre-filled syringe aqueous formulation

	Formulation						Overall (N = 32)
	Lyophilized					Aqueous	
	10 mg (N = 15)	20 mg (N = 31)	30 mg (N = 12)	45 mg (N = 14)	60 mg (N = 13)	20 mg (N = 29)	
All TEAEs	4 (27)	5 (16)	1 (8)	2 (14)	5 (39)	5 (17)	16 (50)
Treatment-related TEAE	3 (20)	4 (13)	0	1 (7)	4 (31)	2 (7)	12 (38)
TEAE leading to discontinuation	0	1 (3)	0	0	1 (8)	1 (3)	3 (9)
Severe TEAEs	0	0	0	0	1 (8)	1 (3)	2 (6)
General disorders and administrative-site conditions							
Injection-site erythema	0	0	0	1 (7)	3 (23)	1 (3)	4 (13)
Injection-site pruritus	1 (7)	1 (3)	0	1 (7)	0	1 (3)	4 (13)
Injection-site induration	0	0	0	1 (7)	1 (8)	1 (3)	3 (9)
Injection-site pain	0	2 (7)	0	0	1 (8)	0	3 (9)
Infections and infestations							
COVID-19	1 (7)	1 (3)	0	0	0	2 (7)	4 (13)
Skin and subcutaneous tissue disorders							
Dermatitis	0	0	1 (8.3)	0	1 (8)	0	2 (6)

Data reported are number of subjects (percentage)

COVID-19 coronavirus disease 2019, TEAE treatment-emergent adverse event

a return to baseline within 48 h. In contrast, SC rusfertide as the lyophilized formulation has a more sustained absorption, with C_{\max} noted approximately 4–24 h following injection and a longer apparent elimination half-life, supporting less frequent dosing. Consistent with the PK profile, rusfertide led to dose-related, rapid, robust, and sustained effects on serum iron and transferrin-iron saturation, with effects noted within 4 h of dose administration. Maximum reductions in serum iron and TSAT were noted approximately 24–48 h following rusfertide administration with a subsequent dose-dependent return to baseline generally at 168 h or later.

VIT-2763, a small-molecule oral ferroportin inhibitor, has a median T_{\max} of 0.5–3 h and a geometric mean elimination half-life of 1.9–5.3 h following single doses in healthy subjects [48]. Correspondingly, the nadir in serum iron levels was observed 4–8 h post-dose, and mean serum iron levels rebounded to baseline or above by 24 h post-dose. The longer duration of effect with rusfertide (nadir at 24 h, which is sustained until 72–96 h) would allow once-weekly or twice-weekly dosing.

This PK and PD trial in healthy subjects guided the choice of the starting dose of 20 mg for the planned phase III safety and efficacy study and ensured patient safety given the demonstrated tolerability of the range of rusfertide exposures previously studied. The similar

relationship between rusfertide exposure (AUC) and serum iron AUEC (Fig. 4) for both formulations suggests that given a desired reduction in serum iron, it would be possible to select the dose of rusfertide required with each formulation.

In phase II studies, SC rusfertide has shown a rapid, robust, and sustained reduction in hematocrit in patients with PV, essentially eliminating the need for phlebotomies [22], an outcome of restricting iron availability for erythropoiesis [49]. These findings in patients with PV are consistent with the PK and PD profile of rusfertide observed in healthy subjects. Rusfertide shows acute reductions in serum iron (Fig. 3A) and an exposure-related decrease in AUEC for serum iron (Fig. 4A), reflecting limited availability of serum iron for erythropoiesis.

Single doses of SC rusfertide doses were generally well tolerated. Approximately 28% of subjects experienced injection-site reactions, with two subjects discontinuing the study early because of these events. No serious AEs were identified in this dose-ranging trial, and no clinically meaningful effects were seen on clinical laboratory parameters, vital signs, or electrocardiograms. The overall safety profile of SC rusfertide was as expected for a hepcidin mimetic intended to limit iron availability.

A limitation of the current study, the presence of low detectable rusfertide concentrations in some subjects in

subsequent treatment periods, was likely a result of the short (2-week) washout period. These instances were generally limited to cases where the previous treatment was 60 mg and the baseline concentration generally comprised less than 7% of the C_{\max} on average. In these cases, the rusfertide plasma concentrations were corrected using an average elimination rate from a previous study with intravenous rusfertide.

5 Conclusions

Results from this single-dose trial in healthy subjects demonstrate that following SC administration, rusfertide is rapidly absorbed, with plasma concentrations noted within 1 h. The lyophilized formulation of rusfertide results in an approximately 1.5-fold higher AUC compared with the aqueous formulation. Pharmacodynamic results in healthy subjects indicate a sustained dose-related and exposure-related effect on limiting systemic availability of iron. Subcutaneous rusfertide was generally well tolerated in healthy subjects, with the most common TEAEs being injection-site reactions.

Supplementary Information The online version contains supplementary material available at <https://doi.org/10.1007/s40268-024-00497-z>.

Acknowledgements We thank Grace Ledet for contributions in developing the lyophilized formulation and Roopa Taranath for determining the activity of the metabolites.

Declarations

Funding The clinical trial was funded by Protagonist Therapeutics, Inc.

Conflict of interest Nishit B. Modi, Sarita Khanna, Sneha Rudraraju, and Frank Valone are current or previous employees or consultants of Protagonist Therapeutics, Inc.

Ethics approval The clinical trial was approved by an independent institutional review board (Advarra) and the trial was performed in accordance with the ethical standards as laid down in the 1964 Declaration of Helsinki and its later amendments.

Consent to participate Informed consent was obtained from all individual participants included in the trial.

Consent for publication Not applicable.

Availability of data and material Anonymized individual patient data may be available upon request or as required by law or regulation with qualified external researchers and demonstrated non-conflict of interest. Approval of such requests is at the discretion of Protagonist Therapeutics, Inc. and is dependent on the nature of the request, the merit of the research proposed, the availability of the data, and the intended use of the data.

Code availability Not applicable.

Author contributions NBM and FHV contributed with the conception and design of the trial, data collection and analyses, and critical manuscript revision; SR contributed to the data analysis; SK contributed to the data analysis, and critical manuscript revision. All authors read and approved the final version.

Open Access This article is licensed under a Creative Commons Attribution-NonCommercial 4.0 International License, which permits any non-commercial use, sharing, adaptation, distribution and reproduction in any medium or format, as long as you give appropriate credit to the original author(s) and the source, provide a link to the Creative Commons licence, and indicate if changes were made. The images or other third party material in this article are included in the article's Creative Commons licence, unless indicated otherwise in a credit line to the material. If material is not included in the article's Creative Commons licence and your intended use is not permitted by statutory regulation or exceeds the permitted use, you will need to obtain permission directly from the copyright holder. To view a copy of this licence, visit <http://creativecommons.org/licenses/by-nc/4.0/>.

References

1. Bennett C, Jackson VE, Pettikiriachchi A, Hayman T, Schaeper U, Moir-Meyer G, et al. Iron homeostasis governs erythroid phenotype in polycythemia vera. *Blood*. 2023;141:3199–214. <https://doi.org/10.1182/blood.2022016779>.
2. James C, Ugo V, Le Couédic J-P, Staerk J, Delhommeau F, Lacout C, et al. A unique clonal JAK2 mutation leading to constitutive signalling causes polycythaemia vera. *Nature*. 2005;434:1144–8. <https://doi.org/10.1038/nature03546>.
3. Mullally A, Lane SW, Ball B, Megerdichian C, Okabe R, Al-Shahrour F, et al. Physiological JAK2V617F expression causes a lethal myeloproliferative neoplasm with differential effects on hematopoietic stem and progenitor cells. *Cancer Cell*. 2010;17:584–96. <https://doi.org/10.1016/j.ccr.2010.05.015>.
4. Marchioli R, Finazzi G, Specchia G, Cacciola R, Cavazzina R, Cilloni D, et al. Cardiovascular events and intensity of treatment in polycythemia vera. *N Engl J Med*. 2013;368:22–33. <https://doi.org/10.1056/NEJMoa1208500>.
5. Marchetti M, Vannucchi AM, Griesshammer M, Harrison C, Koschmieder S, Gisslinger H, et al. Appropriate management of polycythaemia vera with cytoreductive drug therapy: European LeukemiaNet 2021 recommendations. *Lancet Haematol*. 2022;9:e301–11. [https://doi.org/10.1016/S2352-3026\(22\)00046-1](https://doi.org/10.1016/S2352-3026(22)00046-1).
6. NCCN clinical practice guidelines in oncology (NCCN Guidelines®) for myeloproliferative neoplasms V.1.2024.® National Comprehensive Cancer Network, Inc. 2024. Available from: <https://www.nccn.org/guidelines/guidelines-detail?category=1&id=1477>. Accessed 12 Feb 2024.
7. Tefferi A, Barbui T. Polycythemia vera: 2024 update on diagnosis, risk-stratification, and management. *Am J Hematol*. 2023;98:1465–87. <https://doi.org/10.1002/ajh.27002>.
8. Verstovsek S, Pemmaraju N, Reaven NL, Funk SE, Woody T, et al. Real-world treatments and thrombotic events in polycythemia vera patients in the USA. *Ann Hematol*. 2023;102:571–81. <https://doi.org/10.1007/s00277-023-05089-6>.
9. Ganz T. Systemic iron homeostasis. *Physiol Rev*. 2013;93:1721–41. <https://doi.org/10.1152/physrev.00008.2013>.
10. Meynard D, Babitt JL, Lin HY. The liver: conductor of systemic iron balance. *Blood*. 2014;123:168–76. <https://doi.org/10.1182/blood-2013-06-427757>.

11. Park CH, Valore EV, Waring AJ, Ganz T. Hepcidin, a urinary antimicrobial peptide synthesized in the liver. *J Biol Chem*. 2001;276:7806–10. <https://doi.org/10.1074/jbc.M008922200>.
12. Pigeon C, Ilyin G, Courselaud B, Leroyer P, Turlin B, Brissot P, et al. A new mouse liver-specific gene, encoding a protein homologous to human antimicrobial peptide hepcidin, is overexpressed during iron overload. *J Biol Chem*. 2001;276:7811–9. <https://doi.org/10.1074/jbc.M008923200>.
13. Collins JF, Wessling-Resnick M, Knutson MD. Hepcidin regulation of iron transport. *J Nutr*. 2008;138:2284–8. <https://doi.org/10.3945/jn.108.096347>.
14. Nemeth E, Tuttle MS, Powelson J, Vaughn MB, Donovan A, Ward DM, et al. Hepcidin regulates cellular iron efflux by binding to ferroportin and inducing its internalization. *Science*. 2004;306:2090–3. <https://doi.org/10.1126/science.1104742>.
15. Camaschella C, Nai A, Silvestri L. Iron metabolism and iron disorders revisited in the hepcidin era. *Haematologica*. 2020;105:260–72. <https://doi.org/10.3324/haematol.2019.232124>.
16. Ganz T. Hepcidin and iron regulation, 10 years later. *Blood*. 2011;117:4425–33. <https://doi.org/10.1182/blood-2011-01-258467>.
17. Casu C, Nemeth E, Rivella S. Hepcidin agonists as therapeutic tools. *Blood*. 2018;131:1790–4. <https://doi.org/10.1182/blood-2017-11-737411>.
18. Schmidt PJ, Fleming MD. Modulation of hepcidin as therapy for primary and secondary iron overload disorders: preclinical models and approaches. *Hematol Oncol Clin North Am*. 2014;28:387–401. <https://doi.org/10.1016/j.hoc.2013.11.004>.
19. Taranath R, Bourne G, Zhang J, Frederick B, Tran TT, Bhandari A, et al. Hepcidin peptidomimetics: oral efficacy in pre-clinical disease model of iron overload. *Blood*. 2020;136(Suppl. 1):47–8.
20. Taranath R, Mattheakis L, Zhao L, Lee L, Tovera J, Zhao J, et al. Mechanism of systemic iron regulation and hematocrit control by hepcidin peptidomimetics in pre-clinical models. *Blood*. 2020;136(Suppl. 1):49–50.
21. Ginzburg Y, Kirubamoorthy K, Salleh S, Lee S-E, Lee JH, Selvaratnam V, et al. Rusfertide (PTG-300) induction therapy rapidly achieves hematocrit control in polycythemia vera patients without the need for therapeutic phlebotomy. *Blood*. 2021;138(Suppl. 1):390. <https://doi.org/10.1182/blood-2021-149205>.
22. Kremyanskaya M, Kuykendall AT, Pemmaraju N, Ritchie EK, Gotlib J, Gerds A, et al. Rusfertide, a hepcidin mimetic, for control of erythrocytosis in polycythemia vera. *N Engl J Med*. 2024;390:723–35. <https://doi.org/10.1056/NEJMoa2308809>.
23. Ritchie EK, Pettit KM, Kuykendall AT, Kremyanskaya M, Pemmaraju N, Khanna S, et al. Durability of hematocrit control in polycythemia vera with the first-in-class hepcidin mimetic rusfertide: two-year follow up results from the Revive study. *Blood*. 2023;142(Suppl. 1):745.
24. Verstovsek S, Kuykendall A, Hoffman R, Koschmieder S, Passamonti F, Valone F, et al. Verify: a phase 3 study of the hepcidin mimetic rusfertide (PTG-300) in patients with polycythemia vera. *Blood*. 2022;140(Suppl. 1):3929–31.
25. Kowdley KV, Modi NB, Peltekian K, Vierling JM, Ferris C, Valone FH, et al. Rusfertide for the treatment of iron overload in HFE-related haemochromatosis: an open-label, multicentre, proof-of-concept phase 2 trial. *Lancet Gastroenterol Hepatol*. 2023;8:1118–28. [https://doi.org/10.1016/S2468-1253\(23\)00250-9](https://doi.org/10.1016/S2468-1253(23)00250-9).
26. Modi NB, Shames R, Lickliter JD, Gupta S. Pharmacokinetics, pharmacodynamics and tolerability of an aqueous formulation of rusfertide (PTG-300), a hepcidin mimetic, in healthy volunteers: a double-blind first-in-human study. *Eur J Haematol*. 2024;113:340–50. <https://doi.org/10.1111/ejh.14243>.
27. Rathore N, Rajan RS. Current perspectives on stability of protein drug products during formulation, fill and finish operations. *Biotechnol Prog*. 2008;24:504–14. <https://doi.org/10.1021/bp070462h>.
28. Cicerone MT, Pikal MJ, Qian KK. Stabilization of proteins in solid form. *Adv Drug Deliv Rev*. 2015;93:14–24. <https://doi.org/10.1016/j.addr.2015.05.006>.
29. International Council for Harmonisation (ICH). U.S. Department of Health and Human Services. Food and Drug Administration. M10 bioanalytical method validation and study sample analysis. Guidance for industry. November 2022. Available from: <https://www.fda.gov/media/162903/download>. Accessed 28 Jan 2024.
30. National Cancer Institute Division of Cancer Treatment and Diagnosis, Cancer Therapy Evaluation Program. Common terminology criteria for adverse events (CTCAE) v5.0. Available from: https://ctep.cancer.gov/protocoldevelopment/electronic_applications/ctc.htm#ctc_50. Accessed 28 Jan 2024.
31. Gough K, Hutchinson M, Keene O, Byrom B, Ellis S, Lacey L, et al. Assessment of dose proportionality: report from statisticians in the pharmaceutical industry/pharmacokinetics UK joint working party. *Drug Inf J*. 1995;29:1039–48. <https://doi.org/10.1177/009286159502900324>.
32. Smith BP, Vandenhende FR, DeSante KA, Farid NA, Welch PA, Callaghan JT, et al. Confidence interval criteria for assessment of dose proportionality. *Pharm Res*. 2000;17:1278–83. <https://doi.org/10.1023/a:1026451721686>.
33. Gerds AT, Gotlib J, Palmer JM, Pemmaraju N, Bose P, Ginzburg Y, et al. Rusfertide for polycythemia vera: similar dosing in patients receiving therapeutic phlebotomy alone or in combination with cytoreductive treatment. *Blood*. 2022;140(Suppl. 1):12241–3.
34. Jonassen I, Havelund S, Hoeg-Jensen T, Steengaard DB, Wahlund PO, Ribbel U. Design of the novel protraction mechanism of insulin degludec, an ultra-long-acting basal insulin. *Pharm Res*. 2012;29:2104–14. <https://doi.org/10.1007/s11095-012-0739-z>.
35. Havelund S, Ribbel U, Hubálek F, Hoeg-Jensen T, Wahlund PO, Jonassen I. Investigation of the physico-chemical properties that enable co-formulation of basal insulin degludec with fast-acting insulin aspart. *Pharm Res*. 2015;32:2250–8. <https://doi.org/10.1007/s11095-014-1614-x>.
36. Avanti C, Amorij J-P, Setyaningsih D, Hawe A, Jiskoot W, Visser J, et al. A new strategy to stabilize oxytocin in aqueous solutions: I. The effects of divalent metal ions and citrate buffer. *AAPS J*. 2011;13:284–90. <https://doi.org/10.1208/s12248-011-9268-7>.
37. Avanti C, Permentier HP, van Dam A, Poole R, Jiskoot W, Frijlink HW, et al. A new strategy to stabilize oxytocin in aqueous solutions: II. Suppression of cysteine-mediated intermolecular reactions by a combination of divalent metal ions and citrate. *Mol Pharm*. 2012;9:554–62. <https://doi.org/10.1021/mp200622z>.
38. US Food and Drug Administration (FDA), Center for Drug Evaluation and Research. US Department of Health and Human Services. Guidance for industry: safety testing of drug metabolites, 2008. Available from: <https://www.fda.gov/regulatory-information/search-fda-guidance-documents/safety-testing-drug-metabolites>. Accessed 28 Jan 2024.
39. Casu C, Oikonomidou PR, Chen H, Nandi V, Ginzburg Y, Prasad P, et al. Minihepcidin peptides as disease modifiers in mice affected by β -thalassemia and polycythemia vera. *Blood*. 2016;128:265–76. <https://doi.org/10.1182/blood-2015-10-676742>.
40. Casu C, Liu A, De Rosa G, Low A, Suzuki A, Sinha S, et al. Tmprss6-ASO as a tool for the treatment of polycythemia vera mice. *PLoS ONE*. 2021;16: e0251995. <https://doi.org/10.1371/journal.pone.0251995>.
41. Girelli D, Busti F. Manipulating hepcidin in polycythemia vera. *Blood*. 2023;41:3132–4. <https://doi.org/10.1182/blood.2023020509>.
42. Ganz T, Nemeth E, Rivella S, Goldberg P, Dibble AR, et al. Tmprss6 as a therapeutic target for disorders of erythropoiesis

- and iron homeostasis. *Adv Ther.* 2023;40:1317–33. <https://doi.org/10.1007/s12325-022-02421-w>.
43. Porter JB, Scrimgeour A, Martinez A, James L, Aleku M, Wilson R, et al. SLN124, a GalNAc conjugated 19-mer siRNA targeting *tmprss6*, reduces iron and increases hepcidin levels of healthy volunteers. *Am J Hematol.* 2023;98:1425–35. <https://doi.org/10.1002/ajh.27015>.
 44. Lob HE, Ivanova L, Crowell B, Kim H, Idone V, Economides AN, et al. *TMPRSS6* inhibition with a monoclonal antibody improves red blood cell health and reduces hepatic iron loading in mouse models of iron overload diseases. *Blood.* 2022;140(Suppl. 1):8178. <https://doi.org/10.1182/blood-2022-162702>.
 45. Chen B, Wang J, Huang L, Bujold M, Du X. Novel anti-*TMPRSS6* monoclonal antibody provides a potential therapeutic approach for the treatment of polycythemia vera. *Blood.* 2023;142(Suppl. 1):3837. <https://doi.org/10.1182/blood-2023-174782>.
 46. Xiao JJ, Krzyzanski W, Wang Y-M, Li H, Rose MJ, Ma M, et al. Pharmacokinetics of anti-hepcidin monoclonal antibody Ab 12B9m and hepcidin in cynomolgus monkeys. *AAPS J.* 2010;12:646–57. <https://doi.org/10.1208/s12248-010-9222-0>.
 47. Yaeger D, Piga A, Lal A, Kattamis A, Salman S, Byrnes B, et al. A phase 1, placebo-controlled study to determine the safety, tolerability, and pharmacokinetics of escalating subcutaneous doses of LJPC-401 (synthetic human hepcidin) in healthy subjects. Presented at the European Hematology Association 23rd Annual Congress; June 14–17, 2018; Stockholm.
 48. Richard F, van Lier JJ, Roubert B, Haboubi T, Göhring U-M, Dürrenberger F. Oral ferroportin inhibitor VIT-2763: first-in-human, phase 1 study in healthy volunteers. *Am J Hematol.* 2020;95:68–77. <https://doi.org/10.1002/ajh.25670>.
 49. Ginzburg YZ, Feola M, Zimran E, Varkonyi J, Ganz T, Hoffman R. Dysregulated iron metabolism in polycythemia vera: etiology and consequences. *Leukemia.* 2018;32:2105–16. <https://doi.org/10.1038/s41375-018-0207-9>.